24th INTERNATIONAL CONGRESS ON SOUND AND VIBRATION
23–27 July 2017, London

ICSV24
23-27JULY 2017
LONDON CALLING

AN IMPLICIT TIME-DOMAIN FINITE ELEMENT SCHEME FOR SOUND FIELD ANALYSIS WITH PERMEABLE MEMBRANE ABSORBERS

Takeshi Okuzono, Kimihiro Sakagami and Akihiro Katsuyama

Environmental Acoustics Laboratory, Department of Architecture, Graduate School of Engineering, Kobe University, 1-1 Rokkodai-cho, Nada-ku, Kobe 657-8501, Japan
email: okuzono@port.kobe-u.ac.jp

The permeable membrane (PM) absorbers are very attractive from the perspectives of light transmissibility, flexibility and lightweight properties, and various PM absorbers such as single-leaf PM absorbers and PM space absorbers have been proposed based on the theory, experiments and numerical analyses. On the other hand, the applicability of wave-based time domain methods such as finite difference time domain method and time domain finite element method (TDFEM) is increasing gradually for room acoustics design. However, developments of proper absorber models for the time domain analyses are still insufficient. In this paper, a simple and computationally efficient time domain FE model of limp PM absorbers is presented with an implicit TDFEM for sound field analyses with PM absorbers. The applicability is demonstrated through the various problems. First, the validity is shown using impedance tube problems, in which the normal incidence absorption coefficients obtained by the implicit TDFEM are compared with those obtained by theory. Then, the effectiveness of present FE model of PM absorbers is demonstrated through the acoustics simulation of 3D rooms with PM ceiling absorbers. A comparison is performed with an equivalent impedance model to examine the error caused by neglecting the incident angle dependence of surface impedance in the modeling of single-leaf PM absorbers.
Keywords: permeable membrane absorber, finite element method, time domain analysis

1. Introduction

Sound absorbers play an important role for conditioning acoustics in built environments. Among various absorbers, permeable membranes (PM), which are usually made of a core textile coated with resin, have been recognized as one of the attractive absorbing materials thanks to the superior material performances in light transmissibility, flexibility and lightweight properties and so on. Because they have flow resistance suitable for sound absorption purpose, they can absorb the sound energy via acoustic resistance. Various PM absorbers have been proposed and their absorption characteristics were studied using theory, experiments and numerical analyses. The simplest PM absorbers are single-leaf absorbers, in which a PM is placed in front of a rigid wall with an air-cavity in-between. A curtain placed in front of a wall is a simple example of the absorbers. The design theory for rigid and flexible absorbers with and without a honeycomb-backed air cavity can be found in Ref [1], where the PM absorbers are defined as thin porous sheet or screen absorbers. The other recent developments are three-dimensional PM space absorbers [2] for room acoustics application, which can be placed more freely inside rooms, and they also can be combined with a lighting equipment.

On the other hand, for proper room acoustics design, the applicability and practicality of time-domain wave-based methods such as finite difference time domain methods and time domain finite element methods (TDFEM) have advanced significantly in recent year, with the developments of efficient methods. Among the time domain methods, TDFEM has an inherent strength in dealing with complex geometry by the finite element (FE) discretizations of space, and has been applied relative recently to sound field analyses of rooms. In TDFEM, an equivalent impedance model is often used to model absorbers simply [3]. The equivalent impedance model uses a real-valued surface impedance calculated from statistical absorption coefficients based on the locally reacting assumption and it is assumed that the surface impedance is constant in each frequency band. The frequency dependence of absorption coefficient can be considered by calculating the sound field at each frequency band. This model is practically useful because the absorption coefficient database by reverberation room methods can be used. However, for example, the equivalent impedance model might be produced inaccurate results when a surface impedance of absorbers depends strongly on the incidence angle. Therefore, constructing more proper absorber models that can deal with the frequency and incident angle dependence of absorption characteristics is important to increase the accuracy of TDFEM, and such a model can be constructed by dealing with sound propagations inside the absorbers.

In this paper, we present a simple and computationally efficient time domain FE model of PM absorbers that can deal with sound propagations inside absorbers, and also show an implicit TDFEM for sound field analyses in rooms with PM absorbers. First, the theories of time domain FE model of PM and implicit TDFEM are presented together with the equivalent impedance model. Then, the validity is shown through the results of impedance tube problems, in which normal incidence absorption coefficients calculated from the implicit TDFEM are compared with those calculated from the theory [1]. Finally, the difference of results between the proposed time domain FE model and the equivalent impedance model is discussed through sound field analyses in a small rectangular room with a single-leaf PM ceiling absorber.

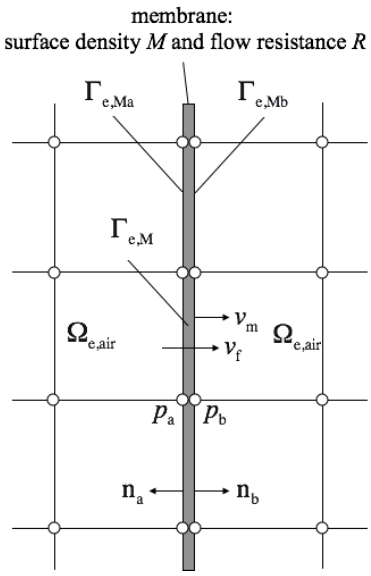

Figure 1: FE model of permeable membrane [4].

2. Theory

2.1 Time domain FE model of PM [4]

We consider limp permeable membranes with no tension. The permeability of PM is expressed by the flow resistance. Figure 1 shows an FE model of a PM with the surface density M and the flow resistance R, in which $\Omega_{e,air}$ and $\Gamma_{e,M}$ respectively represent the air element and PM element

derived with contributions from both boundary surfaces of PM: $\Gamma_{e,Ma}$ and $\Gamma_{e,Mb}$. p_a and p_b represent the sound pressures at the two sides of PM, respectively. v_f and v_m respectively represent the particle velocity near and inside a material, and vibration velocity of PM. n_a and n_b are the normal vectors at a boundary. In the FE model, equation of motion for limp membranes is given as

$$M\dot{v}_m = p_a - p_b \ , \tag{1}$$

where $\cdot$ signify the first-order derivative with respect to time. As for the permeability of PM, the flow resistance can be defined as

$$R = \frac{\dot{p}_a - \dot{p}_b}{\dot{v}_f - \dot{v}_m} \ , \tag{2}$$

with assuming the time factor $\exp(i\omega t)$ where i and ω represent the imaginary unit and the angular frequency. With the Eqs (1) and (2), a PM can be modeled using the following vibration boundary conditions on both boundary surfaces $\Gamma_{e,Ma}$ and $\Gamma_{e,Mb}$.

$$\frac{\partial p}{\partial n} = \begin{cases} -\rho_0 \dot{v}_f & \text{on } \Gamma_{e,Ma} \\ \rho_0 \dot{v}_f & \text{on } \Gamma_{e,Mb} \end{cases} . \tag{3}$$

Here, ρ_0 represents the air density.

2.2 Implicit time domain FEM

We consider a closed sound field with a rigid boundary, a vibration boundary, an impedance boundary and a boundary related to a PM governed by the wave equation. In FEM, FE approximations are introduced to a sound pressure and a weight function in the weak form of the wave equation. Then, considering the all boundary conditions, the semi-discretized matrix equation is given as

$$\mathbf{M}\ddot{\mathbf{p}} + c_0^2\left(\mathbf{K} + \frac{\rho_0}{M}\mathbf{S}\right)\mathbf{p} + c_0\left(\mathbf{C} + \frac{\rho_0 c_0}{M}\mathbf{S}\right)\dot{\mathbf{p}} = \mathbf{f} \ , \tag{4}$$

where **M**, **K** and **C** respectively represent the global mass, stiffness and dissipation matrices. The global matrix **S** represents the contribution of PM. **p** and **f** are the sound pressure vector and the external force vector, respectively. As a direct time integration method, the Newmark β method called Fox-Goodwin method is applied to solve the Eq. (3) in the temporal direction. In this TDFEM, the linear equation at each time step is solved using conjugate gradient iterative solver with diagonal scaling preconditioning. The convergence tolerance is set to 10^{-6}.

2.3 Equivalent impedance model

The equivalent impedance model uses a real-valued equivalent impedance z_e calculated from statistical absorption coefficients by Paris' formula based on the locally reacting assumption. Also, in time domain analyses, it is assumed that the impedance is constant in frequency range of interest. The frequency dependence of absorption characteristics can be modeled by calculating time responses at each frequency band. For the calculations, we can use a band-limited impulse response of digital filter as a sound source. With the assumption that z_e is independent of incidence angle, the Paris' formula is given as [5]

$$\bar{\alpha}_e = \frac{8}{z_e^2}\left[1 + z_e - \frac{1}{1+z_e} - 2\ln(1+z_e)\right], \tag{5}$$

where $\bar{\alpha}_e$ represents the statistical absorption coefficient. The subscript e indicates the use of z_e. In Eq. (5), measured reverberant absorption coefficients can be used as an approximate value of statistical absorption coefficients as well as theoretically calculated statistical absorption coefficients for

various absorbers. The advantage of using the equivalent impedance model is that we can use sufficiently accumulated database in reverberation absorption coefficients of various absorbers.

3. Validation with impedance tube problem

To show the validity of the present TDFEM for sound field analyses with PM absorbers, impedance tube problems with single-leaf PM absorbers were analyzed and calculated absorption coefficients at normal incidence were compared with those calculated by theory [1].

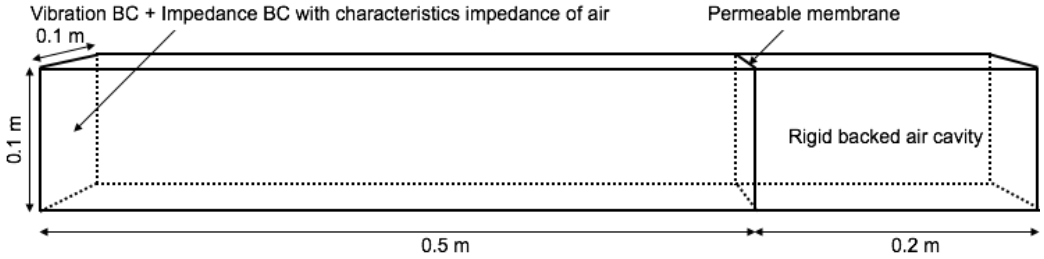

Figure 2: Three dimensional impedance tube model for FE analyses.

3.1 Impedance tube problem

Figure 2 shows the impedance tube model for three dimensional FE analyses, where PMs with different material properties in the surface density and the flow resistance were placed in front of a rigid wall with an air cavity of 0.2 m depth. Considering the material properties of existing PMs [2], the following three PMs were used for the simulation; (a) PM A : M = 0.065 kg/m^2 and R = 196 Pa s/m, (b) PM B : M = 0.120 kg/m^2 and R = 462 Pa s/m, and (c) PM C : M = 0.495 kg/m^2 and R = 1087 Pa s/m. The surface impedances of respective PM absorbers were calculated directly from the sound pressure and the particle velocity on the absorber surface. Then, the normal incidence absorption coefficients were calculated. In the FE analyses, a modulated Gaussian pulse was used as a sound source, which was given as vibration acceleration waveform on the surface of tube end. Also, the surface has the characteristic impedance of air, to avoid a reflection. The upper-limit frequency was assumed as 1.5 kHz. Acoustic FEs used here is eight node hexahedral elements with modified integration rules [6] to reduce a dispersion error. The PM was also modeled using eight node hexahedral PM elements. Three FE meshes (Mesh 1 ~ Mesh 3) with different spatial resolutions were used to confirm the convergence of results. The spatial resolution λ/h of Mesh 1 ~ Mesh 3 are respectively 4.6, 9.2 and 18.3 at the upper-limit frequency, where λ and h respectively represent the wavelength and the maximum element length. For respective FE meshes, time intervals were set to 1/12,000 s (Mesh 1), 1/24,000 s (Mesh 2) and 1/48,000 s (Mesh 3), respectively.

3.2 Absorption characteristics of single-leaf PM absorbers

According to the Ref [1], the surface impedance of purely resistive single-leaf PM absorbers with non-locally reacting rigid-backed air cavity can be expressed as

$$z_{\mathrm{n}} = \left(\frac{\rho_0 c_0}{R} + \frac{\rho_0 c_0}{i\omega M} \right)^{-1} - \frac{i}{\cos\theta} \cot\left(kL\cos\theta \right) , \tag{6}$$

where L represents air cavity depth. The first and second terms respectively represent the transfer impedance of PM and the reactance of non-locally reacting air cavity. Note that the non-locally reacting air cavity is mainly responsible for the frequency dependence of surface impedance. The oblique incidence absorption coefficient α_θ is calculated as

$$\alpha_\theta = \frac{4\,\mathrm{Re}\left[z_{\mathrm{n}} \right]\cos\theta}{\left(\mathrm{Re}\left[z_{\mathrm{n}} \right]\cos\theta + 1 \right)^2 + \left(\mathrm{Im}\left[z_{\mathrm{n}} \right]\cos\theta \right)^2} . \tag{7}$$

Using α_θ, the statistical absorption coefficient is obtainable as

$$\alpha_s = 2\int_0^{\pi/2} \alpha_\theta \cos\theta \sin\theta \, d\theta \ . \tag{8}$$

3.3 Comparison of FEM with conventional theory

Figures 3(a) ~ 3(c) respectively show comparisons of normal incidence absorption coefficients α_0 calculated using TDFEM with Mesh 1 ~ 3 and theory. Overall, α_0 s calculated using TDFEM are in good agreement with those obtained by theory, irrespective of used Meshes and material properties of PM, and converged solutions were obtained for Mesh 2 and 3. Only for the results of Mesh 1, which is the coarsest mesh, slight discrepancies can be found at around 1.5 kHz due to the dispersion error. Numerical results showed that the present TDFEM can analyze the absorption characteristics of PM absorbers.

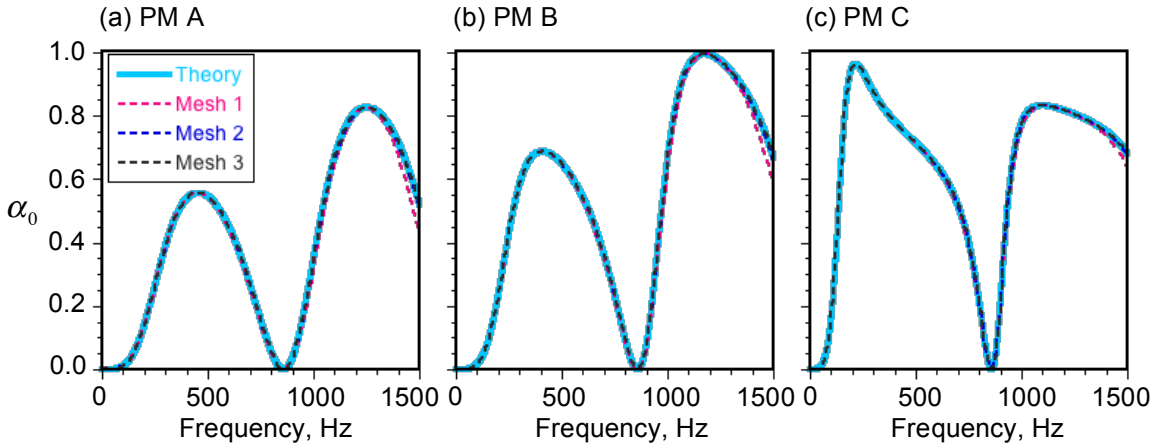

Figure 3: Comparison of normal incidence absorption coefficients between TDFEM with three FE meshes and theory; (a) PM A, (b) PM B and (c) PM C.

4. Comparison with equivalent impedance model

As shown in the Eq. (6), the surface impedance of single-leaf PM absorbers has an incident angle dependence due to the effect of non-locally reacting air cavity, whereas the equivalent impedance model neglects the dependence. In this section, to demonstrate the effectiveness of the presented FE model, the error comes from the use of equivalent impedance model is briefly shown.

4.1 Analyzed sound field

The sound fields in a small rectangular room with a single-leaf PM ceiling absorber were analyzed using the present FE model of PM and the equivalent impedance model. Other boundaries except in the ceiling are reflective boundaries. Figures 4(a) and 4(b) show the analyzed sound field with a source point and 12 receiving points. The PM C was used for the ceiling absorber, and the oblique incidence coefficients of absorber calculated using Eq. (6) are shown in the Fig. 4(c). In the equivalent impedance model, equivalent impedance z_e was calculated using Eq. (5) at each octave band, where α_s calculated from Eqs. (6)-(8) was substituted into Eq. (5) as $\bar{\alpha}_e$. Figure 4(c) also shows the oblique incidence absorption coefficients by the equivalent impedance model. We computed band-limited impulse responses (IR) with octave bandwidths of center frequencies 125 Hz, 250 Hz, 500 Hz and 1 kHz. The sound source is the impulse responses of IIR filter. The acoustic FEs and PM elements used here are the same as previous section. The DOFs in FE meshes for both models are 876225 for the present model and 840000 for the equivalent impedance model.

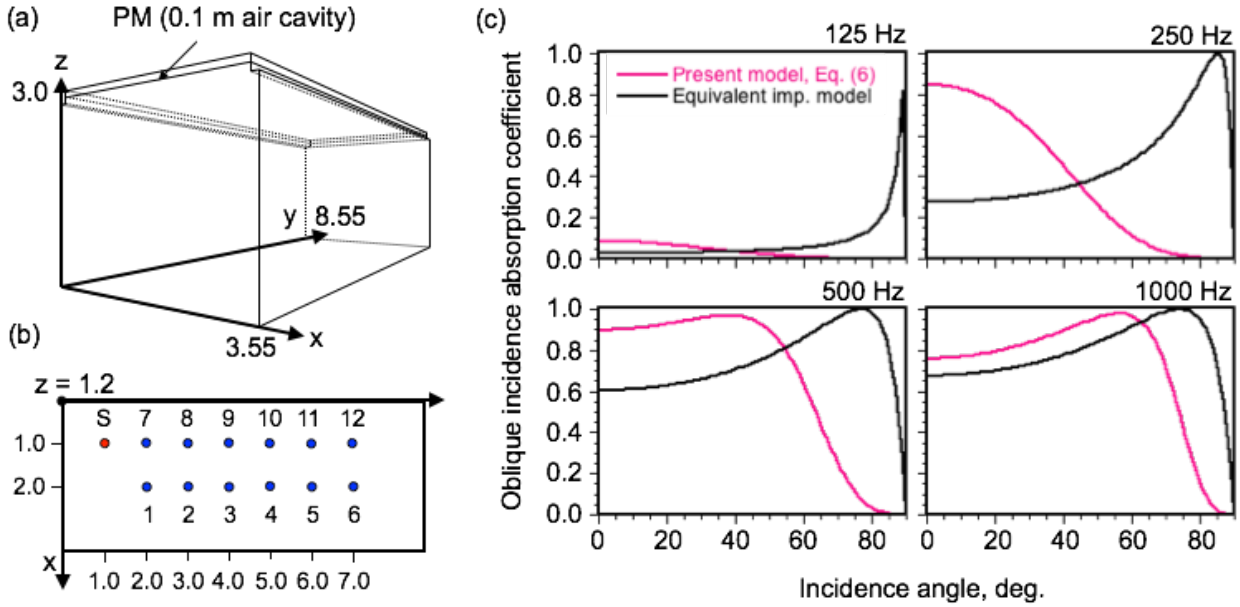

Figure 4: (a) Small rectangular room with single-leaf PM ceiling absorber, (b) Source and receiving points, and (c) Oblique incidence absorption coefficients of present model and equivalent impedance model.

4.2 Results and discussion

Figure 5 and 6 respectively show the comparisons of band-limited IRs and corresponding decay curves at a receiving point R4 between the present model and the equivalent impedance model at each frequency. It also includes results for case without the absorber. Overall, the band-limited IRs of equivalent impedance model show larger decay than those of the presented FE model except for the results at 125 Hz due to the small absorption coefficient of PM absorber. However, at 125 Hz, fine structure of IRs calculated using the present FE model and the equivalent impedance model is different in early time region. Significant difference can be found at 250 Hz. The reason of difference can be explained as follows. As shown in Fig. 4(c), oblique incidence absorption coefficients of the present model become smaller as incident angle increases, whereas those of the equivalent impedance model show the opposite trend exactly. In addition, this sound field has reflective floor and side walls, and the single-leaf PM absorber has low grazing incidence absorption coefficients as shown in Fig. 4(c). Therefore, as in the results of present model in Fig. 6, the reverberation decay of the sound field would show the slow decay due to the slow decay of axial and tangential modes in the horizontal direction, i.e., the sound field becomes a non-diffuse sound field [7]. However, the equivalent impedance model shows high grazing incidence absorption coefficients, and accordingly, the reverberation decay shows larger decay than the presented FE model as in the Fig. 6. The result showed that the difference of incident angle dependence of surface impedance gives significant influence on a decay process though the statistical absorption coefficients are the same in the both models.

At mid frequencies, the discrepancies in decay curves between the two models become smaller as frequency increases. At the frequencies, the oblique incidence absorption coefficients between the two models show the similar incidence angle dependence characteristics, as shown in the Fig. 4(c), i.e., the incidence angle dependence of surface impedance due to the non-locally reacting air cavity becomes smaller at higher frequencies. Further, at mid frequencies, the slow decay of the axial and tangential modes in the horizontal direction is enhanced than low frequencies because the wavelength becomes relatively shorter compared to the room's height [8]. The equivalent impedance model shows consequently the slow decay as in the present model although the equivalent impedance model has larger absorption coefficients at larger incident angles. These might be the reason of the smaller discrepancies between the two models at mid frequencies.

As for the computational cost of the two models, their computational times at 1 kHz were respectively 5309 s for the present FE model and 4793 s for the equivalent impedance model. The increase of computational time by using the present model is trivial, and it can be said that the present model is computationally efficient.

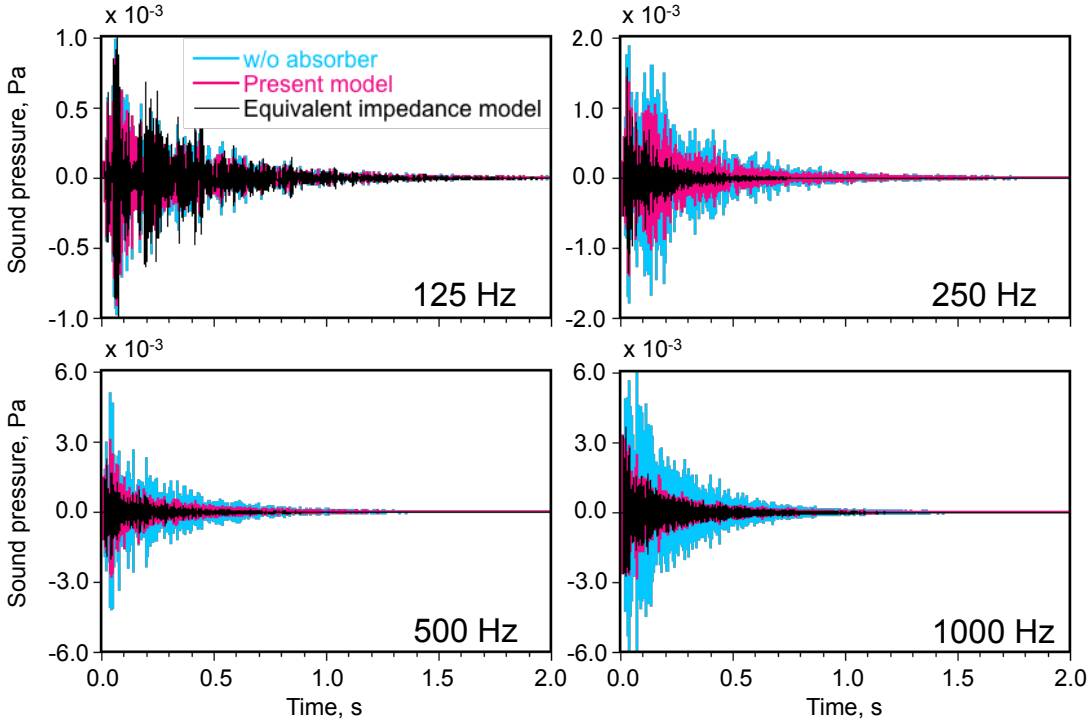

Figure 5: Comparison of band-limited impulse responses at a receiving point R4 between present model and equivalent impedance model. Results for the case without absorber are also presented.

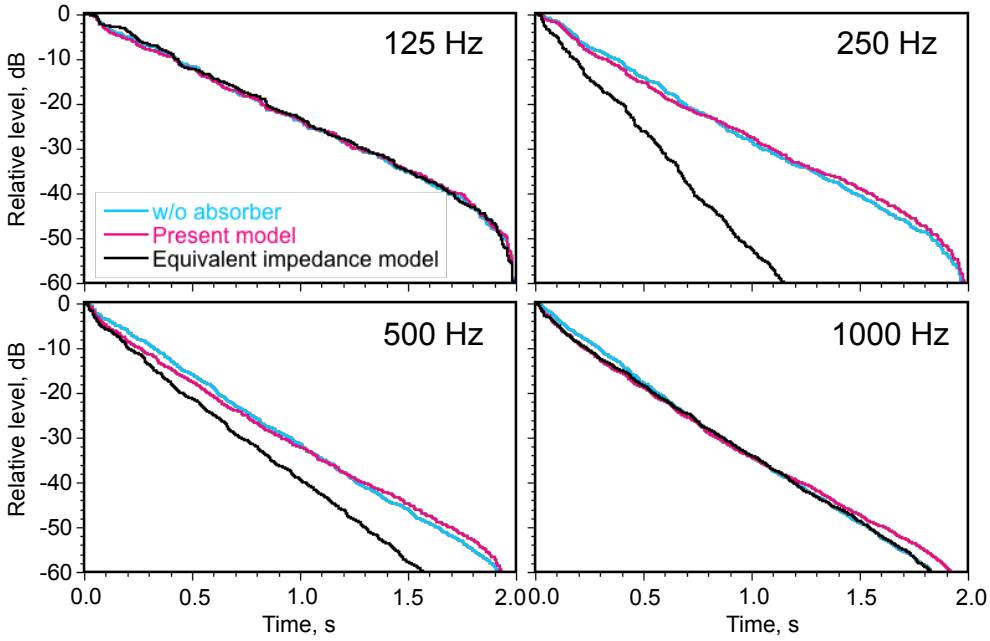

Figure 6: Comparison of decay curves at a receiving point R4 between present model and equivalent impedance model. Results for the case without absorber are also presented.

5. Concluding remarks

This paper presented a simple and computationally efficient time domain FE model of PM absorbers that can deal with sound propagations inside absorbers, and an implicit TDFEM for sound field analyses with PM absorbers is also shown. The validity was confirmed through the results of the impedance tube problems, where the FEM solutions converged to theoretical absorption coefficients using the mesh with proper spatial resolution. Further, the effectiveness of present FE model was demonstrated through the sound field analyses in a small rectangular room with a single-leaf PM ceiling absorber. The numerical results showed that the incident angle dependence in surface impedance is not negligible for modeling single-leaf PM absorbers, and the use of equivalent impedance model leads to large errors at low frequencies in the presented case.

Acknowledgments

This work was supported in part by JSPS KAKENHI Grant No. 15K18167. The computation was partly conducted using the computer facilities at the Research Institute for Information Technology, Kyushu University.

REFERENCES

1 Ingard, U. *Notes on sound absorption technology*, Noise Control Foundation, New York, USA, Chapter 1, 1–16 (1994).

2 Sakagami, K., Funahashi, K., Somatomo Y., Okuzono, T., Niahikawa, C. and Toyoda, M. An experimental study on the absorption characteristics of a three-dimensional permeable membrane space sound absorber, *Noise Control Engineering Journal*, **63** (3), 300–307, (2015).

3 Okuzono, T., Otsuru, T., Tomiku, R. and Okamoto, N. Fundamental accuracy of time domain finite element method for sound-field analysis of rooms, *Applied Acoustics*, **71** (10), 940–946, (2010).

4 Okuzono, T. and Sakagami, K. A time-domain finite element model of permeable membrane absorbers, *Acoustical Science and Technology*, **37** (1), 46–49, (2016).

5 London, A. The determination of reverberant sound absorption coefficients from acoustics impedance measurements, *The Journal of the Acoustical Society of America*, **22** (2), 263–269, (1950).

6 Okuzono, T., Otsuru, T., Tomiku, R. and Okamoto, N. Application of modified integration rule to time-domain finite-element acoustic simulation of rooms, *The Journal of the Acoustical Society of America*, **132** (2), 804–813, (2012).

7 Nilsson, E. Decay processes in rooms with non-diffuse sound fields Part I: Ceiling treatment with absorbing material, *Building Acoustics*, **11** (1), 39–60, (2004).

8 Yasuda, Y., Ushiyama, A., Sakamoto, S. and Tachibana, H. Experimental and numerical studies on reverberation characteristics in a rectangular room with unevenly distributed absorbers, *Acoustical Science and Technology*, **27** (6), 366–374, (2006).